LASER ABLATION INDUCTIVELY COUPLED PLASMA MASS SPECTROMETRY AND RAMAN SPECTROSCOPY IMAGING OF BIOLOGICAL TISSUES

Emma Lee Gorishek, B.S.

Thesis Prepared for the Degree of

MASTER OF SCIENCE

UNIVERSITY OF NORTH TEXAS

May 2016

APPROVED:

Guido F. Verbeck, IV, Major Professor
William E. Acree, Jr., Committee Member
Samuel Tenney, Committee Member

Gorishek, Emma Lee. *Laser Ablation Inductively Coupled Plasma Mass Spectrometry and Raman Spectroscopy Imaging of Biological Tissues.* Master of Science (Chemistry-Analytical Chemistry), May 2016, 43 pp., 2 tables, 9 figures, references, 132 titles.

Laser Ablation Inductively coupled plasma mass spectrometry (LA-ICP-MS) and Raman spectroscopy are both powerful imaging techniques. Their applications are numerous and extremely potential in the field of biology. In order to improve upon LA-ICP-MS an in-house built cold cell was developed and its effectiveness studied by imaging *Brassica napus* seeds. To further apply LA-ICP-MS and Raman imaging to the field of entomology a prong gilled mayfly (Ephemeroptera: Leptophlebiidae) from the Róbalo River, located on Navarino Island in Chile, was studied. Analysis of both samples showcased LA-ICP-MS and Raman spectroscopy as effective instruments for imaging trace elements and larger molecules in biological samples respectively.

ACKNOWLEDGMENTS

First and foremost, I would like to express my thanks and gratitude for my advisor, Dr. Guido F. Verbeck, IV. Without his aid and support, not only in my graduate career but also through my undergraduate studies, I would have been unable to complete this project. I would like to thank my other committee members, Dr. William Acree, Jr and Dr. Samuel Tenney for their support through my graduate career. Thank you to the UNT Chemistry Department for the teaching opportunities and support. I would like to thank my fellow group members, current and graduated, whose friendship, support, and effort helped push me further. Thank you to my dear friends for supporting me with love and enthusiasm. Mom and Dad, you made a point to instill the importance of education in me and helped to fan the flames for my love of chemistry and the sciences. Thank you for your tireless support, without you I would have never made it to this point. To Erin, Liz, and Emily watching you three grow with excitement for your respective sciences and pursue your education with such tenacity has helped drive me forward. To Cale, you have always been my number one fan and head cheerleader. Thank you for listening to me through phone and skype calls as I studied and worked through the night.

TABLE OF CONTENTS

Page

LIST OF TABLES AND FIGURES

Tables

Figures

ABBREVIATIONS LIST

B. napus	*Brassica napus*
CRI	Collision/Reaction Interface
FT-IR	Fourier Transform Infrared Spectroscopy
ICP-MS	Inductively Coupled Mass Spectrometry
LA	Laser Ablation
LA-ICP-MS	Laser Ablation Inductively Couple Mass Spectrometry
LDI	Laser Desorption/Ionization
MALDI	Matrix-Assisted Laser Desorption/Ionization
RF	Radio-frequency
SIMS	Secondary Ion Mass Spectrometry

CHAPTER 1

INTRODUCTION

"A picture is worth a thousand words."

The visualization of the chemistry contained within a biological sample in situ is a simple method of understanding the functions of a biological system, physiology, localization of specific chemistry, or even the effect of chemistry on the biological system. Imaging displays the chemical information of a sample in a method that is easy to understand and correlate to the physical features. The chemistry imaged can range from atomic, compounds, sugars, lipids, peptides, and is only limited by the instrumentation selected. There are many methods and forms of instrumentation that can be used to image such samples. Fluorescence, Raman, Fourier transform infrared (FT-IR) are examples of spectroscopic imaging techniques. As well as a multitude of imaging mass spectrometry techniques such as Secondary Ion Mass Spectrometry (SIMS), Laser Desorption/Ionization (LDI), Matrix-Assisted Laser Desorption/Ionization (MALDI), and Laser Ablation Inductively Coupled Plasma Mass Spectrometry (LA-ICP-MS).[1] The following thesis will discuss the application of LA-ICP-MS and Raman spectroscopy imaging to biological samples such as plant matter and invertebrates. As well as address the importance of cold cell techniques with LA-ICP-MS.

---

* Parts of this chapter have been previously published in part from J. S. Hamilton, E. L. Gorishek, P. M. Mach, D. Strutevant, M. L. Ladage, N. Suzuki, P. A. Padilla, R. Mitler, K. D. Chapman, G. F. Verbeck, *J. Anal. At. Spectrom.,* **2016**, 31, 1030-1033.

1.1 Selected Methods of Imaging

1.1.1 Laser Ablation Inductively Coupled Mass Spectrometry

Typically for a sample to be analyzed by inductively coupled plasma mass spectrometry (ICP-MS) it must first be subjected to various methods of digestion and cleaning in order to be measurable by the instrument.[2] As a method of bypassing such needs laser ablation (LA) has been coupled with ICP-MS so that solid samples may be analyzed. LA-ICP-MS, first described by Gray in 1985, has proven to be a useful tool not only for the analysis of solid samples but imaging them as well.[3] Applications of LA-ICP-MS have shown that the analytical technique is capable of both the bulk analysis of homogenous solids[4-10] and the spatially resolved elemental distributions of heterogeneous proteins of 2D gels,[11-16] and intact solid samples.[17-24] More specifically, spatially resolved elemental imaging of biological tissues has been demonstrated using a plethora of biological material including: animal brain,[25-35] cells,[36,37] hair,[38-42] kidney,[43-47] liver,[48-52] tumors[53-57] among other tissues[58-61]; as well as, flower petals,[62,63] leaves[64,65] and roots;[66,67] in addition to whole *Caenorhabditis elegans*,[68,69] and full cross sections of slugs[70,71] and sea snails.[72] Sample selection for LA-ICP-MS is only limited by ablation cell size and/or the prolonged integrity of the sample during analysis.

With LA-ICP-MS imaging elements and their isotopes is possible on the trace and even ultratrace level along with many more advantages. It allows for in situ analysis of metals and non-metals in solid tissue samples.[73] This method of imagining is sensitive, ppm to ppt range, with precise spatially resolved measurements from about 10-100 μm[74,75] with a full spatial resolution range of 5-200 μm.[76] Depending on the sample and element analyzed, it has proven to be a reproducible method with reproducibility values

ranging from 5-8%.[77] Quantitative imaging is possible so long as matrix matching is taken into account, such as NIST standard leaves doped with a known concentration of analyte to compare to sample leaves, or and in laboratory made matrix matched standard can be made or solution-based calibration may be used.[73,78] There is little to no sample prep needed and thin tissue section can be measured, only small samples are needed, and there is a low risk of contamination.[76]

LA-ICP-MS is not without its problems. Due to the nature of ICP, only elements and isotopes may be analyzed, not compounds. To abide with the proper timing with laser shots and analysis time only a few elements, around five or so given method development, can be analyzed at a time. While there are limited matrix effects, the matrix of the sample must still be considered in order for quantification to be done.[77] LA is a destructive technique, as a laser is used to either mostly or entirely ablate the sample. With high water content of the tissues coupled with the heating induced by the laser a change in the nature of the surface being ablated can be witnessed. This causes the transient signal to be instable and analytical errors to be introduced. This issue can be combatted by a cooled ablation cell, which reduces the heat degradation of the tissue.[79,80]

1.1.2 Raman Spectroscopy

Raman imaging offers an efficient and intuitive means of visualizing material properties of heterogeneous samples in a nondestructive and noninvasive manner. As most, if not all, biological samples are heterogeneous in nature, Raman is an extremely useful tool.

There are many biological applications to Raman imaging. From biomedical applications of tumor in tissues such as brain and breast, effects of diseases in the gastrointestinal tract, colon, bladder, kidneys, prostate, skin, even retinas. Studies have also been done that utilize Raman imaging to study drug uptake in cellular systems, insects set in resin,[81] chitin and chitosan,[82,83] globin in *Aphrodite aculeate*,[84] and meiofauna.[85]

1.2 References

1. M. L. Reyzer and R. M. Caprioli, The Development of Imaging Mass Spectrometry, In The Encyclopedia of Mass Spectrometry, Elsevier, Boston, **2016**, Pages 285-304.
2. Thomas, R. *Practical Guide to ICP-MS;* Marcel Dekker, Inc.: New York, NY, **2004**
3. Gray, A. L. Solid Sample Introduction by Laser Ablation for Inductively Coupled Plasma Source Mass Spectrometry. *Analyst*, **1985***, 110*, 551.
4. D. R. Bandura, O. I. Ornatsku and L. Liao, *Journal of Analytical Atomic Spectrometry*, **2004**, 19, 96-100.
5. T. Punshon, B. P. Jackson, P. M. Bertsch and J. Burger, *Journal of Environmental Monitoring*, **2004**, 6, 153-159.
6. M. D. Seltzer and K. H. Berry, *Science of the Total Environment*, 2005, 339, 253-265.
7. J. Shi, M. A. Gras and W. K. Silk, *Planta*, **2009**, 229, 945-954.
8. A. Hanc, D. Baralkiewicz, A. Piechalak, B. Tomaszewska, B. Wagner and W. Bulska, *International Journal of Environmental Analytical Chemistry*, **2009**, 89, 651-659.
9. I. Cakmak, M. Kalayci, Y. Kaya, A. A. Torun, N. Aydin, Y. Wang, A. Arisoy, H. Erdem, A. Yazici, O. Gokmen, L. Ozturk and W. J. Horst, *Journal of Agricultural and Food Chemistry*, **2010**, 58, 9092-9102.

10. L. YS, H. ZC, L. M and G. S, *Chinese Science Bulletin*, **2013**, 58, 3863-3878.
11. G. Ballihaut, C. Pecheyran, S. Mounicou, H. Preud'homme, R. Grimaud and R. Lobinski, *Trends in Analytical Chemistry*, **2007**, 26, 183-190.
12. A. Polatajko, M. Azzolini, I. Feldmann, T. Stuezel and N. Jakubowski, *Journal of Analytical Atomic Spectrometry*, **2007**, 22.
13. J. S. Becker, S. Mounicou, M. V. Zoriy, J. S. Becker and R. Lobinski, *Talanta*, **2008**, 76.
14. J. S. Becker, M. Zoriy, B. Wu, A. Matusch and J. S. Becker, *Journal of Analytical Atomic Spectrometry*, **2008**, 23, 1275-1280.
15. J. S. Becker, R. Lobinski and J. S. Becker, *Metallomics*, **2009**, 312-316.
16. G. Ballihaut, L. E. Kilpatrick, E. L. Kilpatrick and W. C. Davis, *Journal of Analytical Atomic Spectrometry*, **2011**, 26, 383-394.
17. J. S. Becker and J. S. Becker, *Mass Spectrometry Imaging: Imaging of metals, metalloids, and non-metals by laser ablation inductively coupled plasma mass spectreomtry (LA-ICP-MS) in biological tissues*, **2010**.
18. J. S. Becker, A. Matusch, J. S. Becker, B. Wu, C. Palm, A. J. Becker and D. Salber, *International Journal of Mass Spectrometry*, **2011**, 307, 3-15.
19. Wu and J. S. Becker, *International Journal of Mass Spectrometry*, **2011**, 307, 112-122.
20. V. L. Dressler, F. G. Antes, C. M. Moreira, D. Pozebon and F. A. Duarte, *International Journal of Mass Spectrometry*, **2011**, 307, 149-162.
21. Z. Qin, J. A. Caruso, B. Lai, A. Matusch and J. S. Becker, *Metallomics*, **2011**, 3, 28-37.
22. I. Konz, B. Fernandez, M. L. Fernandez, R. Pereiro and A. Sanz-Medel, *Analytical and Bioanalytical Chemistry*, **2012**, 403, 2113-2125.
23. O. Reifschneider, C. A. Wehe, I. Raj, J. Ehmcke, G. Ciarimboli, M. Sperling and U. Karst, *Metallomics*, **2013**, 5, 1440-1447.
24. C. A. Wehe, G. M. Thyssen, C. Herdering, I. Raj, G. Ciarimboli, M. Sperling and U. Karst, *Journal of the American Society for Mass Spectrometry*, **2015**.
25. B. Jackson, S. Harper, L. Smith and J. Flinn, *Analytical and Bioanalytical Chemistry*, **2006**, 384, 951-957.

26. J. S. Becker, J. S. Becker, M. V. Zoriy, J. Dobrowlska and A. Matusch, European *Journal of Mass Spectrometry*, **2007**, 13, 1-6.
27. M. V. Zoriy and J. S. Becker, *International Journal of Mass Spectrometry*, **2007**, 264, 175-180.
28. J. S. Becker, M. Zoriy, J. S. Becker, J. Dobrowolska and A. Matusch, *Journal of Analytical Atomic Spectrometry*, **2007**, 22, 736-744.
29. J. Dobrowolska, M. Dehnhardy, A. Matusch, M. Zoriy, N. Palomero-Gallagher, P. Koscielniak, K. Zilles and J. S. Becker, *Talanta*, **2008**, 74, 717-723.
30. J. S. Becker, H. Sela, J. Dobrowolska, M. Zoriy and J. S. Becker, *International Journal of Mass Spectrometry*, **2008**, 270, 1-7.
31. D. Hare, B. Reedy, R. Grimm, S. Wilkins, I. Volitakis, J. L. George, R. A. Cherny, A. I. Bush, D. I. Finkelstein and P. Doble, *Metallomics*, **2009**, 1, 53-58.
32. A. Matusch, C. Depboylu, C. Palm, B. Wu, G. U. Hoglinger, M. K.-H. Schafer and J. S. Becker, *Journal of the American Society for Mass Spectrometry*, **2010**, 21, 161-171.
33. J. S. Becker, *International Journal of Mass Spectrometry*, **2010**, 289, 65-75.
34. A. Matusch, A. Bauer and J. S. Becker, *International Journal of Mass Spectrometry*, **2011**, 307, 240-244.
35. A. Sussulini and J. S. Becker, *Talanta*, **2015**, 132, 579-582.
36. D. Drescher, C. Giesen, H. Traub, U. Panne, J. Kneipp and N. Jakubowski, *Analytical Chemistry*, **2012**, 84, 9684-9688.
37. L. Mueller, H. Traub, N. Jakubowski, D. Drescher, V. I. Baranov and J. Kneipp, *Analytical and Bioanalytical Chemistry*, **2014**, 406, 6963-6977.
38. M. Legrand, R. Lam, M. Jensen-Fontaine, E. D. Salin and H. M. Chan, *Journal of Analytical Atomic Spectrometry*, **2004**, 19, 1287-1288.
39. H. Sela, Z. Karpas, M. Zoriy, C. Pickhardt and J. S. Becker, *International Journal of Mass Spectrometry*, **2007**, 261, 199-207.
40. D. Pozebon, V. L. Dressler, A. Matusch and J. S. Becker, *International Journal of Mass Spectrometry*, **2008**, 272, 57-62.
41. V. L. Dressler, D. Pozebon, M. F. Mesko, A. Matusch, U. Kumtabtim, B. Wu and J. S. Becker, *Talanta*, **2010**, 82, 1770-1777.

42. U. Kumtabtim, A. Matusch, S. U. Dani, A. Siripinyanond and J. S. Becker, *International Journal of Mass Spectrometry*, **2011**, 307, 185-191.
43. J. Feldman, A. Kindness and P. Elk, *Journal of Analytical Atomic Spectrometry*, **2002**, 17, 813-818.
44. M. Zoriy, A. Matusch, T. Spruss and J. S. Becker, *International Journal of Mass Spectrometry*, **2007**, 260, 102-106.
45. E. Moreno-Gordaliza, C. Giesen, A. Lazaro, D. Esteban-Fernandez, b. Humanes, B. Canas, U. Panne, A. Tejedor, N. Jakubowski and M. M. Gomez-Gomez, *Analytical Chemistry*, **2011**, 23, 7933-7940.
46. M. Birka, K. S. Wentker, E. Lusmoller, B. Arheilger, C. A. Wehe, M. Sperling, R. Stadler and U. Karst, *Analytical Chemistry*, **2015**, 87, 3321-3328.
47. S. heiner, C. Kornauth, K. P. Varbanov, M. Galanski, S. V. Schoonhoen, P. Heffeter, W. Berger, A. E. Egger and B. K. Keppler, *Metallomics*, **2015**, 7, 1256-1264.
48. A. Kindness, C. N. Sekaran and J. Feldman, *Clinical Chemistry*, **2003**, 49, 1916-1923.
49. N. C. Sekaran, *Current Science*, **2006**, 90, 221-225.
50. B. D. Barst, A. K. Gevertz, M. M. Chumchal, J. D. Smith, T. R. Rainwater, P. E. Drevnick, K. E. Hudelson, A. Hart, G. F. Verbeck and A. P. Roberts, *Environmental Science and Technology*, **2011**, 45, 8982-8988.
51. P. M-M, R. Weiskirchen, N. Gassler, A. K. Bosserhoff and J. S. Becker, *PLOS One*, **2013**, 8.
52. P. M-M, U. Merle, R. Weiskirchen and J. S. Becker, *International Journal of Mass Spectrometry*, **2013**, 354-355, 281-287.
53. J. S. Becker, M. V. Zoriy, M. Dehnhardt, C. Pickhardt and K. Zilles, *Journal of Analytical Atomic Spectrometry*, **2005**, 20, 912-917.
54. M. V. Zoriy, M. Dehnhardy, G. Reifenberger, K. Zilles and J. S. Becker, *International Journal of Mass Spectrometry*, **2006**, 257, 27-33.
55. M. V. Zoriy, M. Dehnhardt, A. Matusch and J. S. Becker, *Spectrochimica Acta Part B*, **2008**, 63, 375-382.

56. D. Hare, S. Tolmachev, A. James, D. Bishop, C. Austin, F. Fryer and P. Doble, *Analytical Chemistry*, **2010**, 82, 3176-3182.
57. O. Reifschneider, C. A. Wehe, K. Diebold, C. Becker, M. Sperling and U. Karst, *Journal of Analytical Atomic Spectrometry*, **2013**, 28, 989-993.
58. B. P. Jackson, W. A. Hopkins and J. Biaonno, *Environmental Science and Technology*, **2003**, 37, 2511-2515.
59. D. Kang, D. Amarasiriwardena and A. H. Goodman, *Analytical and Bioanalytical Chemistry*, **2004**, 378, 1608-1615.
60. I. Konz, B. Fernandez, M. L. Fernandez, R. Pereiro and H. Gonzalez-Iglesias, *Analytical and Bioanalytical Chemistry*, **2014**, 406, 2343-2348.
61. S. Bohme, H.-J. Stark, D. Kuhnel and T. Reemtsma, *Analytical and Bioanalytical Chemistry*, **2015**, 407, 5477-5485.
62. J. S. Becker, A. Gorunoff, M. Zoriy, A. Izmer and M. Kayser, *Journal of Analytical Atomic Spectrometry*, **2006**, 21, 19-25.
63. J. Kaiser, M. Galiova, K. Novotny, R. Cervenka, L. Reale, J. Novotny, M. Liska, O. Samek, V. Kanicky, A. Hrdlicka, K. Stejskal, V. Adam and R. Kizek, *Spectrochimica Acta Part B*, **2009**, 64, 67-73.
64. B. Wu, M. Zoriy, Y. Chen and J. S. Becker, *Talanta*, **2009**, 78, 132-137.
65. B. Wu, Y. Chen and J. S. Becker, *Analytica Chimica Acta*, **2009**, 633, 165-172.
66. A. B. Moradi, S. Swoboda, B. Robinson, T. Prohaska, A. Kaestner, S. E. Oswald, W. W. Wenzel and R. Schulin, *Environmental and Experimental Botany*, **2010**, 69, 24-31.
67. B. Wu, I. Susnea, Y. Chen, M. Przybylski and J. S. Becker, *International Journal of Mass Spectrometry*, **2011**, 307, 85-91.
68. S. G. Brinkhaus, J. Bornhorst, S. Chakraborty, C. A. Wehe, R. Niehaus, O. Reifschneider, M. Aschner and U. Karst, *Metallomics*, **2014**, 6, 617-621.
69. B. Crone, M. Aschner, T. Schwerdtle, U. Karst and J. Bornhorst, *Metallomics*, **2015**, 7, 1189-1195.
70. J. S. Becker, A. Matusch, C. Depboylu, J. Dobrowolska and M. V. Zoriy, *Analytical Chemistry*, **2007**, 79, 6074-6080.

71. J. S. Becker, D. Pozebon, A. Matusch, V. L. Dressler and J. S. Becker, *International Journal of Mass Spectrometry*, **2011**, 307, 66-69.
72. M. C. Santos, M. Wagner, B. Wu, J. Scheider, J. Oehlmann, S. Cadore and J. S. Becker, *Talanta*, **2009**, 80, 428-433.
73. Wu, B.; Zoriy, M.; Chen, Y.; Becker, J. S. Imaging of nutrient elements in the leaves of Elsholtzia splendens by laser ablation inductively coupled plasma mass spectrometry (LA-ICP-MS). *Talanta* **2009***, 78*, 132-137.
74. Matusch, A.; Depboylu, C.; Palm, C.; Wu, B.; Höglinger, G. U.; Schäfer, M. K. -.; Becker, J. S. Cerebral Bioimaging of Cu, Fe, Zn, and Mn in the MPTP Mouse Model of Parkinson's Disease Using Laser Ablation Inductively Coupled Plasma Mass Spectrometry (LA-ICP-MS). *J. Am. Soc. Mass Spectrom.* **2010***, 21*, 161-171.
75. Becker, J. S.; Matusch, A.; Wu, B. Bioimaging mass spectrometry of trace elements – recent advance and applications of LA-ICP-MS: A review. *Anal. Chim. Acta* **2014***, 835*, 1-18.
76. Becker, J. S. Bioimaging of metals in brain tissue from micrometre to nanometre scale by laser ablation inductively coupled plasma mass spectrometry: State of the art and perspectives. *International Journal of Mass Spectrometry* **2010***, 289*, 65-75.
77. Zoriy, M. V.; Becker, J. S. Imaging of elements in thin cross sections of human brain samples by LA-ICP-MS: A study on reproducibility. *International Journal of Mass Spectrometry* **2007***, 264*, 175-180.
78. Wu, B.; Chen, Y.; Becker, J. S. Study of essential element accumulation in the leaves of a Cu-tolerant plant Elsholtzia splendens after Cu treatment by imaging laser ablation inductively coupled plasma mass spectrometry (LA-ICP-MS). *Anal. Chim. Acta* **2009***, 633*, 165-172.
79. Konz, I.; Fernández, B. F.; Fernández, M. L.; Pereiro, R.; Sanz-Medel, A. Design and evaluation of a new Peltier-cooled laser ablation cell with on-sample temperature control. *Analytica Chimica Acta* **2014**, 88.
80. Zoriya, M. V.; Kayserb, M.; Izmera, A.; Pickhardta, C.; Becker, J. S. Determination of uranium isotopic ratios in biological samples using laser

ablation inductively coupled plasma double focusing sector field mass spectrometry with cooled ablation chamber. *International Journal of Mass Spectrometry* **2005**, 297.

81. H. G.M. Edwards, D. W. Farwell, S. E. J. Villar, *Spectrochimica Acta Part A: Molecular and Biomolecular Spectroscopy*, **2007**, 68, 1089-1095.
82. A. Zając, J. Hanuza, M. Wandas, L. Dymińska, *Spectrochimica Acta Part A: Molecular and Biomolecular Spectroscopy*, **2015**, 134, 114-120.
83. C. V. Serrano, H. Leemreize, B. Bar-On, F. G. Barth, P. Fratzl, E. Zolotoyabko, Y. Politi, *Journal of Structural Biology*, **2016**, 193, 124-131.
84. K. Ramser, W. Wenseleers, S. Dewilde, S. Van Doorslaer, L. Moens, D. Hanstorp, *Journal of Biochemical and Biophysical Methods*, **2007**, 70, 627-633.
85. L. C. Maurin, D. Himmel, J. Mansot, O. Gros, *Marine Environmental Research*, **2010**, 5, 382-389.

CHAPTER 2

INSTRUMENTATION

2.1 Materials

Brassica napus seeds (courtesy of Dr. Kent Chapman and Drew Strutevant) were set in 10% (w/v) porcine gelatin (Sigma Aldirch; St. Louis, MO) in 18.2MΩ H2O (Millipore, Billerica, MA). The seed slices were exposed to nitrocellulose paper (Bio-Rad; Hercules, CA), and rinsed with Optima methanol (Fisher Scientific, Fair Lawn, NJ). Prong-gilled mayflies (courtesy of Dr. James Kennedy, sourced from Róbalo River, Navarino Island, Chile) were set in 10% (w/v) bovine gelatin (Sigma Aldirch; St. Louis, MO) in 18.2MΩ H2O. The samples were sliced using a CM1950 cryostat (Leica Biosystems; Waverley, Australia) and thaw mounted on 18x18mm 1 ounce glass coverslips (Thermo Scientific; Waltham, MA). Bright field images of both sample types sliced, *B. napus* seeds and prong-gilled mayflies, were taken on an AZ100 microscope (Nikon; Melville, NJ). The inductively coupled mass spectrometric analysis was performed on a 820-MS ICP (Bruker (formerly Varian, INC.); Billerica, MA) coupled with an UP-213 laser ablation system (Electro Scientific Industries (formerly New Wave Research); Portland, OR). The Raman spectroscopic imaging was performed on an IHR550 Raman Imaging Spectrometer with Synapse detector (HORIBA Scientific; Edison, NJ) with a 785 nm laser source (Innovative Photonic Solutions, Fat Boy Laser Module; Monmouth Junction, NJ) mounted to an inverted TE2000U microscope (Nikon; Melville, NJ).

2.2 Inductively Coupled Mass Spectrometry Instrumentation

Initially developed as a spectroscopy technique, ICP has been coupled with mass spectrometry and utilized as an effective and extremely sensitive method of trace analysis with detection limits in the picogram range.

2.2.1 Ionization Source

In an attempt to find the ideal plasma source for spectrometric instruments ICP was developed as one of the answers. As seen in figure 1, the ICP consists of a torch made of three concentric tubes with a radio-frequency (RF) coil around the end of the torch. The plasma gas, which is typically argon, flows through the compartment between the outer and middle tube and feeds the plasma at ~12-17 L/min. In order to form the plasma a tangential flow of argon streams between the outer and middle tube and an alternating current of 740-1500 W is applied to the RF coil at a frequency of 27 to 40 MHz.

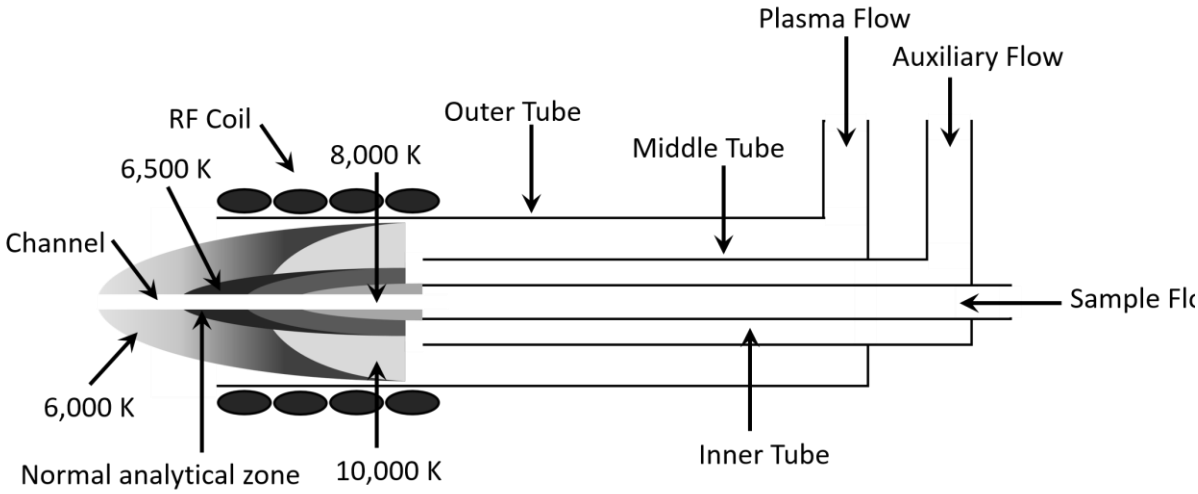

Figure 1: Schematic of an inductively coupled plasma torch with temperature regions of the plasma labeled.

A high-voltage spark strips the electrons from their argon atoms and the electrons are then contained within the electromagnetic field formed at the top of the torch by the oscillating RF current. Trapped by the field the electrons accelerate and collide with other argon atoms to further strip more electrons thus forming the plasma. The auxiliary gas, a second gas flow but same as what is used for the plasma, passes between the middle and inner tube at ~1 L/min. Within the inner tube the nebulizer gas which contains the aerosolized sample flows through at ~1 L/min. The flow of the nebulizer causes a channel to form through the middle of the plasma. The sample undergoes a multi-step process once it enters preheating region of the plasma. In the case of a liquid sample it first undergoes desolvation as the water molecules in the droplet evaporate. The solid sample is then vaporized, atomized as a gas, and finally ionized.[1]

$$M(H_2O)^1X^2 \rightarrow (MX)_n \rightarrow MX \rightarrow M \rightarrow M^1$$

Droplet (Desolvation) Solid (Vaporization) Gas (Atomization) Atom (Ionization) Ion

Figure 2: Mechanism of ion formation in an inductively coupled plasma, starting from droplet desolvation to ionization.

2.2.2 Ion Optics

While ICP-MS is considered to have superior detection capabilities it is plagued with slew of problems that cause low efficiency. Such issues include space charge effects caused by matrix elements from the sample being of a higher concentration than the analyte and the introduction of photons and solid particles from the plasma which would increase the noise if directed to the detector. Ion optics are therefore included before the

mass analyzer to prevent this problems. The form of ion optics utilized by the ICP-MS used includes an ion mirror with a hollow structure and set orthogonal to the mass analyzer. Photons, neutrals, and solid particles pass through the hollow structure and into the vacuum pump behind the mirror. With the mirror orthogonal the ions are refocused by the parabolic electrostatic field formed and reflected at a 90° angle to the mass analyzer. This method of ion focusing is efficient, decreases the chance of contamination, and increases the sensitivity of the instrument. Along with the orthogonal ion mirror the ICP-MS also utilizes off-axis octopole fringe rods post ion mirror. The fringe rods optimize the transmission of ions by a mass-dependent RF voltage which lowers the background levels.[1]

2.2.3 Mass Analyzer

The most common mass analyzer utilized in ICP-MS are quadrupoles.[1] First introduced by Wolfgang Paul in the 1950s, quadrupoles consist of four either perfectly similar circular rods or hyperbolic section. In order to separate ions both a direct current and time-dependent alternating current radio frequency are applied on opposite pairs of rods. Selected masses are able to travel through the quadrupole to the detector when the ideal AC/DC potential is set while all other masses will not be stable and will leave the quadrupole.[2]

2.2.4 Collision/Reaction Interface

Due to the high temperature nature of the plasma along with the combination of argon, solvent, and matrix-derived ions polyatomic interferences that form post ionization are an issue with quadrupole based systems. There are not many elements with poor detection limits, but those that do exist are mainly due to these interferences. For

example, $^{56}Fe^{+}$ is interfered by $^{40}Ar^{16}O^{+}$ and $^{40}Ca^{+}$ is interfered by $^{40}Ar^{+}$. To combat these interferences Collision/Reaction Interface (CRI) can be implemented to eliminate the formation of such interferences. CRI systems work by streaming gas, usually H_2, directly into the plasma through channels in the sampler and skimmer cone interface between the plasma and ion guide system. The H_2 collisions with argon gas in the high-density, high-temperature environment of the plasma destroys or prevents the formation of the polyatomic interference species and thus once they reach the ion mirror they are removed as neutrals instead of directed into the quadrupole.[1]

$$H_2 + {}^{40}Ar^{+} = Ar + H_2^{+}$$

$$H_2 + {}^{56}Fe^{+} = {}^{56}Fe^{+} + H_2 \text{ (no reaction)}$$

Figure 3: Example of the Collision/Reaction Interface process with $^{56}Fe^{+}$ and $^{40}Ar^{+}$.

2.2.5 Laser Ablation

Typically for a solid sample to be analyzed by ICP-MS it must first be subjected to various methods of digestion and cleaning preparation1 to be measurable by the instrument as an aqueous sample. As a method of bypassing lengthy preparation steps, LA has been coupled with ICP-MS so that solid samples may be directly analyzed. First described by Gray in 1985,[3] LA-ICP-MS has proven to be a versatile instrument.[4-23] LA-ICP-MS utilizes a laser to ablate the sample and a secondary gas, usually helium, to sweep the ablation into the plasma. A major benefit of LA-ICP-MS is that it requires little to no sample preparation allowing for the use of intact and/or native state solid samples during analysis. With that ability, LA-ICP-MS has swiftly developed into an elemental

mapping technique allowing for the imaging of metals in the sample. Imaging with LA-ICP-MS is done using a line scanning method. The laser ablates across the raster line at a speed to match the chosen spot size. From an XYZ matrix of the intensity data of a selected element a contour color map is generated.[1]

2.2.6 Cold Cell

While many solid samples are rigid in structure, many temperature dependent, soft-, and semi-soft tissues can undergo fundamental changes at the surface due to laser induced heating effects during ablation. Various custom ablation cells have been developed to overcome this issue including liquid nitrogen cooled cells and cryogenically cooled cells.[24-26] The method of cooling selected utilizes a Peltier element and flowing ice water. The custom made cell was constructed to fit the UP-213 laser system (New Wave Research, Freemont, CA). The cooled cell consists of an acetal housing (Figure 4A) fitted with an adjustable acetal standoff (Figure 4C) to support the heat sink.(Figure 4D) The heat sink is a custom hollow copper block with two piping extensions to pump liquid coolant through the block. The single Peltier thermoelectric element (Marlow Industries, NL2064T- 11AB, Dallas, TX) is affixed directly on top of the heat sink (Figure 4E) with thermally conductive grease to ensure efficient heat transfer from the Peltier device to the copper cooling block. Temperature of the ablation cell is monitored using a PT-111 platinum resistance thermometer connected to a LakeShore 218 Temperature Monitor (LakeShore Cryotronics, Inc., Westerville, OH). Samples are placed on glass cover slips set directly onto the Peltier element for ablation (Figure 4B). Ice water is pumped through the copper heat sink, and replenished as needed, via a small Amico priming diaphragm pump (Amico Power Corp., Baldwin Park, CA). The cold cell and the commercial cell

hold the same dimensions, 75.58mm x 81.19mm x 55.09mm, meaning no alterations were made to the UP-213 laser system.[27]

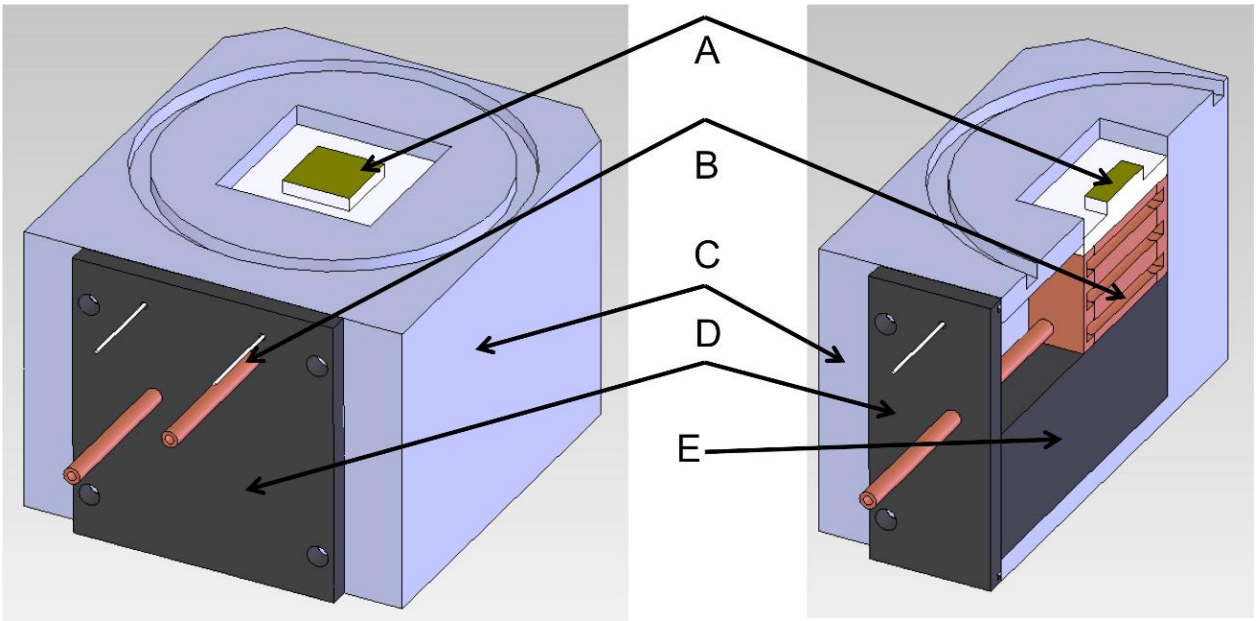

Figure 4: This is a schematic representation of the Peltier cooler based Cold Stage Block. Within the actual housing (A) the spacing block (C) is in place to support the copper-cooling block (D) and the Peltier Cooling Device (E). The copper-cooling block is a hollow block with an inlet and outlet tube which allow water to be pumped through the block. The inlet and outlet tubes of the copper cooling block as well as the leads for the Peltier Cooling device pass through the face plate (B).

2.3 Raman Spectroscopy Instrumentation

With the use of an intense monochromatic beam of electromagnetic radiation, Raman spectroscopy is the measurement of the inelastic scattering of radiation by the

sample. Due to the energy transfer between the photons and the molecular vibrations, the scattered photons have a different energy than the incoming photons. The excitation causes an induced dipole moment which can be split into 3 components known as Stokes, anti-Stokes, and Rayleigh scattering. Rayleigh scattering has the same outgoing frequency as the ingoing photon. Anti-Stokes scattering exhibits a higher energy than the incident beam and Stokes scattering is lower energy.[28]

In order to image with Raman spectroscopy, the sample is analyzed using a point-by-point scanning method. The laser is focused on a small spot on the sample, the spectrum is collected, and then the stage moves to the next spot on the sample along the raster line until the analysis is complete. There are many benefits to Raman imaging. It is nondestructive and nonintrusive which can allow for the study of biological systems without worry of harm or the ability to further analyze chosen samples with other methods post Raman analysis.[29]

2.4 References

1. R. Thomas, *Practical Guide to ICP-MS: A Tutorial For Beginners*, **2008**, 23-91.
2. E. de Hoffmann, V. Stroobant, *Mass Spectrometry: Principles and Applications*, **2007**, 85-91
3. A. L. Gray, *Analyst*, 1985, **110**, 551-556.
4. P. M. Outridge, G. Veinott and R. D. Evans, *Environmental Reviews*, **1995**, 3, 160-170.
5. S. F. Durrant, *Journal of Analytical Atomic Spectrometry*, **1999**, 14, 1385-1403.
6. D. Gunther, S. E. Jackson and H. P. Longerich, *Spectrochimica Acta Part B*, **1999**, 54, 381-409.
7. J. S. Becker, *Spectrochimica Acta Part B*, **2002**, 57, 1805-1820.
8. D. Gunther and B. Hattendorf, *Trends in Analytical Chemistry*, **2005**, 24, 255-264.
9. S. F. Durrant and N. I. Ward, *Journal of Analytical Atomic Spectrometry*, **2005**, 20.
10. C. Pickhardt, H.-J. Dietze and J. S. Becker, *International Journal of Mass Spectrometry*, **2005**, 242, 273-280.
11. R. Lobinski, C. Moulin and R. Ortega, *Biochimie*, 2006, **88**, 1591-1604.
12. B. Fernandez, F. Claverie, C. Pecheyran and O. F. X. Donard, *Trends in Analytical Chemistry*, **2007**, 26, 951-966.
13. A. A. Ammann, *Journal of Mass Spectrometry*, **2007**, 42, 419-427.
14. J. L. Burguera and M. Burguera, *Spectrochimica Acta Part B*, **2009**, 64, 451-458.
15. J. S. Becker and N. Jakubowski, *Chemical Society Reviews*, **2009**, 38, 1969-1983.
16. J. Pisonero, B. Fernandez and D. Gunther, *Journal of Analytical Atomic Spectrometry*, **2009**, 24, 1145-1160.
17. J. S. Becker, M. Zoriy, A. Matusch, B. Wu, D. Salber, C. Palm and J. S. Becker, *Mass Spectrometry Reviews*, **2010**, 29, 156-175.
18. J. S. Becker, A. Matusch, C. Palm, D. Salber, K. A. Morton and J. S. Becker, *Metallomics*, **2010**, 2, 104-111.
19. J. S. Becker, *Journal of Mass Spectrometry*, **2013**, 48, 255-268.
20. S. R. Ellis, A. L. Bruinen and R. M. A. Heeren, *Analytical and Bioanalytical Chemistry*, **2014**, 406, 1275-1289.

21. J. S. Becker, A. Matusch and B. Wu, *Analytica Chimica Acta*, **2014**, 835, 1-18.
22. D. Pozebon, G. L. Scheffler, V. L. Dressler and M. A. G. Nunes, *Journal of Analytical Atomic Spectrometry*, **2014**, 29, 2204-2228.
23. K. Jurowski, B. Buszewski and W. Piekoszewski, *Talanta*, **2015**, 131, 273-285.
24. H. Reinhardt, M. Kriews, H. Miller, O. Schrems, C. Ludke, E. Hoffmann, J. Skole, *Fresen. J. Anal. Chem.*, **2001**, 370, 629-636.
25. R. Kessel, P. Ulmer, T. Pettke, M. W. Schmidt, A. B. Thompson, *Am. Mineral.*, **2004**, 89, 1078-1086.
26. J. Feldman, A. Kindness, P. Elk, *J. Anal. Atom. Spectrom.*, **2002**, 17, 813-818.
27. G. F. Verbeck, W. D. Hoffman. *US Pat.*, US8586943 B2, **2012**.
28. P. Vandenabeele, *Practical Raman Spectroscopy: An Introduction*, **2013**, 1-38.
29. S. Šašić, Y. Ozaki, *Raman, Infrared, and Near-Infrared Chemical Imaging*, **2010**, 23-26.

CHAPTER 3

NORMAL VERSUS COLD LA-ICP-MS IMAGING OF *Brassica napus* SEED

3.1 Introduction

First described by Gray in 1985,[1] LA-ICP-MS as an analytical method has since been extensively reviewed applied to many areas of research. More specifically, spatially resolved elemental imaging of biological tissues has been demonstrated using a plethora of biological material such as animal tissues[2-20] and tumors.[21-25] As well as plant material, for example leaves,[26,27] roots,[28,29] and flower petals.[30,31]

LA-ICP-MS is beneficial due to the fact that it requires little to no sample preparation, meaning samples can remain intact and in their native state during analysis without the need of dissolving and solution prep.[1,32-35] However, many temperature dependent, soft-, and semi-soft tissues can undergo fundamental changes at the surface due to laser induced heating effects during ablation.[36] Cryogenic ablation cells cooled by liquid nitrogen (LN2) have been developed for spatially resolved elemental analysis of ice cores,[37] diamond-trap experiments,[38] oil samples,[39] and biological tissues.[40] It has been reported that the LN2 cryo-cells produce unstable temperatures[41] that affect O-ring integrity[40] and can be considered too cold, while the Peltier-cooled cells have better temperature control, via applied voltage adjustments.[41] Peltier elements have been implemented into custom cooled ablation cell with metal sample stages designs by Becker et al.,[42,43] Aerts et al.,[41] Konz et al.,[44] and Hannigan et al..[45] Our group has

---

* Parts of this chapter have been previously published in part from J. S. Hamilton, E. L. Gorishek, P. M. Mach, D. Strutevant, M. L. Ladage, N. Suzuki, P. A. Padilla, R. Mitler, K. D. Chapman, G. F. Verbeck, *J. Anal. At. Spectrom.,* **2016**, 31, 1030-1033.

developed a new Peltier cooled ablation cell without the use of a sample stage that is a direct replacement for the UP-213 laser system's ablation cell from New Wave Research, based upon previous work.[39] In order to evaluate the benefit of the in house made cooled ablation cell Brassica napus seed slices were analyzed both with the cooled cell and without.

3.2 Experimental

3.2.1 Sample Prep

Mature desiccated seeds were embedded in 10% (w/v) porcine gelatin in 18.2MΩ H2O. The embedded seeds were frozen at -80°C for 24 hours and transferred to -20°C for 72 hours to equilibrate. Sections were cryo-cut with a Leica CM1950 at -18°C at 20µm and thaw mounted on 18x18mm 1 ounce glass coverslips which range from 0.13–0.17mm thickness. After sectioning, the tissues were lyophilized for 24 hours then stored in a desiccator. Seed slices were exposed to nitrocellulose paper for 24 hours, rinsed with optima grade methanol (0.07% water max), and nitrogen dried before imaging.

3.2.2 Laser Ablation Conditions and Cell Run Procedure

The sample-mounted coverslip is then placed on top of the Peltier device and loaded into the ablation chamber, and locked into place creating an air tight seal. In the case of the cold analyzed sample, a voltage, between 1.0V – 1.8V, is then applied to the Peltier device while ice water is pumped through the heat sink. The ambient temperature analysis was performed without the application of voltage to the Peltier device and flow of ice water. The ablation chamber is then purged with helium, the carrier gas, at a rate of 1000 mL/min and this flow remains during the cool down of the sample to prevent

condensation build-up while the Peltier device reaches the desired temperature. The LA-ICP-MS imaging of tissues at room temperature is performed using the same ablation chamber and Peltier device, however, no voltage is applied to the Peltier device and ambient temperature water is pumped through the heat sink. The UP-213's CCD camera is used to focus the laser relative to the surface of the sample to determine the Z-position of the line-by-line raster pattern. ICP and Laser settings were set according to Table 1. A XYZ color map of each selected element is then generated from the intensity data obtained.

ICP Parameters		**Laser Settings**	
Rf Power	1.5 kW	Wavelength (nm)	213
Plasma Flow	16.5 L/min	Ablation mode	Line by line
Analytes	^{31}P, ^{55}Mn	Repetition Frequency (Hz)	20
		Number of Passes	1
		Energy output	90%
Analysis Mode	Semi-Quantitative, Time resolved, Peak hopping	Spot diameter (µm)	40
		Scan speed (µm/s)	40
		Distance between lines	35

Table 1: Laser and ICP parameters and settings used in this experiment.

3.3 Results/Discussion

To evaluate the benefit of cold cell ablation versus ambient temperature ablation *Brassica napus* seeds were ablated at both temperatures (Figure 5). The presence of ^{31}P is expected to be found throughout the cell due to its importance in the seed[46] while the micronutrient ^{55}Mn is expected to be localized in specific areas of the seed.[47] Therefore, both signals were monitored to provide spatially resolved data of an abundant element compared to a less abundant and more localized element within the seed. By comparison, the cooled ablation images show better resolution and improved localization of the monitored elements. This is noted by the higher clarity of the cooled images. More specifically, the ^{31}P is found to be rather homogenously dispersed throughout the seed, with an increase abundance in the seed coat relative to the interior of the seed. Alternatively, the ^{55}Mn is localized within the exterior of the seed coat and within the interior of the seed, but not throughout the entire seed. The improved image quality is due to less water vapor build up when using the cold cell as compared to the commercial cell. Therefore, the use of the single Peltier-cooled ablation cell provides better spatially resolved image as compared to the ambient ablation method.

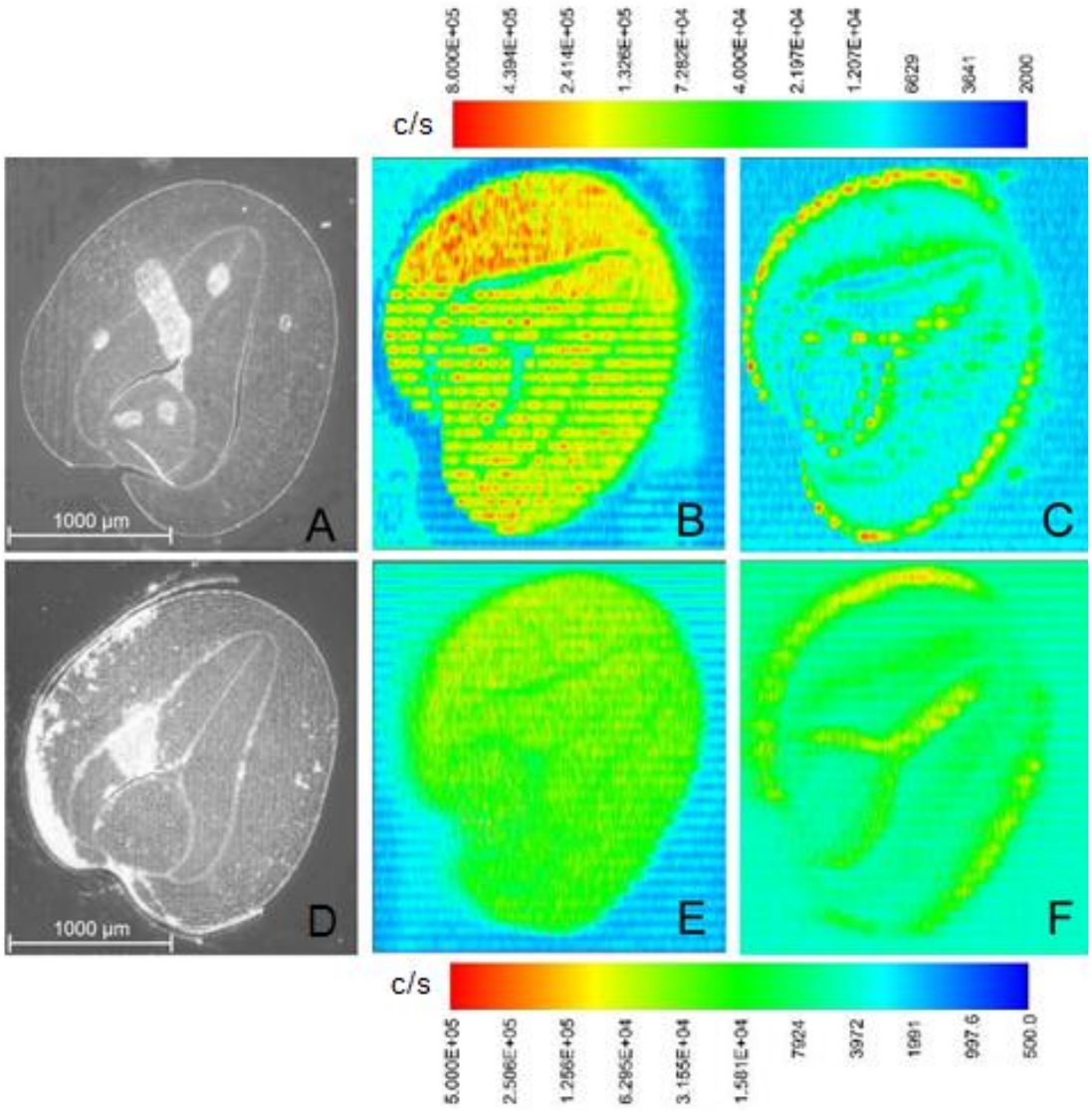

Figure 5: Top: (A) CCD pre-ablation image of B. napus seed section, cooled ablation of 31P (B) and 55Mn (C). Bottom: (D) CCD pre-ablation image of B. napus seed section, normal ablation of 31P (E) and 55Mn (F) Differences in orientation between the CCD images and elemental images are due to shifts in placement when moving the seed to microscope after ablation. Artefacts in the images are due to the line scan method.[48]

3.4 Conclusion

In conclusion, the single Peltier element design of a new cooled laser ablation cell has shown to provide spatially resolved elemental imaging capabilities of biological samples through LA-ICP-MS. The simplicity of this design is significant in that fewer materials are used while still performing well in the experiments presented here; as well as inferring that, fewer components equates to easier repair and maintenance of the device. By placing only a glass coverslip between the cooling element and a sample there is less energy required to cool the sample as compared to other devices because less area needs to be cooled to achieve desired temperatures. With ice water pumping through the copper block biological temperatures were held at a temperature sufficient to maintain their structural integrity. Lower temperatures may be achieved by pumping other liquid coolants through the device if future work requires.

3.5 References

1. A. L. Gray, *Analyst*, **1985**, 110, 551-556.
2. B. Jackson, S. Harper, L. Smith and J. Flinn, *Analytical and Bioanalytical Chemistry*, **2006**, 384, 951-957.
3. J. S. Becker, J. S. Becker, M. V. Zoriy, J. Dobrowlska and A. Matusch, *European Journal of Mass Spectrometry*, **2007**, 13, 1-6.
4. M. V. Zoriy and J. S. Becker, *International Journal of Mass Spectrometry*, **2007**, 264, 175-180.
5. J. S. Becker, M. Zoriy, J. S. Becker, J. Dobrowolska and A. Matusch, *Journal of Analytical Atomic Spectrometry*, **2007**, 22, 736-744.
6. J. Dobrowolska, M. Dehnhardy, A. Matusch, M. Zoriy, N. Palomero-Gallagher, P. Koscielniak, K. Zilles and J. S. Becker, *Talanta*, **2008**, 74, 717-723.
7. J. S. Becker, H. Sela, J. Dobrowolska, M. Zoriy and J. S. Becker, *International Journal of Mass Spectrometry*, **2008**, 270, 1-7.
8. D. Hare, B. Reedy, R. Grimm, S. Wilkins, I. Volitakis, J. L. George, R. A. Cherny, A. I. Bush, D. I. Finkelstein and P. Doble, *Metallomics*, **2009**, 1, 53-58.
9. A. Matusch, C. Depboylu, C. Palm, B. Wu, G. U. Hoglinger, M. K.-H. Schafer and J. S. Becker, *Journal of the American Society for Mass Spectrometry*, **2010**, 21, 161-171.
10. J. S. Becker, *International Journal of Mass Spectrometry*, **2010**, 289, 65-75.
11. A. Matusch, A. Bauer and J. S. Becker, *International Journal of Mass Spectrometry*, **2011**, 307, 240-244.
12. A. Sussulini and J. S. Becker, *Talanta*, **2015**, 132, 579-582.
13. E. Moreno-Gordaliza, C. Giesen, A. Lazaro, D. Esteban-Fernandez, b. Humanes, B. Canas, U. Panne, A. Tejedor, N. Jakubowski and M. M. Gomez-Gomez, *Analytical Chemistry*, **2011**, 23, 7933-7940.
14. M. Birka, K. S. Wentker, E. Lusmoller, B. Arheilger, C. A. Wehe, M. Sperling, R. Stadler and U. Karst, *Analytical Chemistry*, **2015**, 87, 3321-3328.

15. S. heiner, C. Kornauth, K. P. Varbanov, M. Galanski, S. V. Schoonhoen, P. Heffeter, W. Berger, A. E. Egger and B. K. Keppler, *Metallomics*, **2015**, 7, 1256-1264.
16. A. Kindness, C. N. Sekaran and J. Feldman, *Clinical Chemistry*, **2003**, 49, 1916-1923.
17. N. C. Sekaran, *Current Science*, **2006**, 90, 221-225.
18. B. D. Barst, A. K. Gevertz, M. M. Chumchal, J. D. Smith, T. R. Rainwater, P. E. Drevnick, K. E. Hudelson, A. Hart, G. F. Verbeck and A. P. Roberts, *Environmental Science and Technology*, **2011**, 45, 8982-8988.
19. P. M-M, R. Weiskirchen, N. Gassler, A. K. Bosserhoff and J. S. Becker, *PLOS One*, **2013**, 8.
20. P. M-M, U. Merle, R. Weiskirchen and J. S. Becker, *International Journal of Mass Spectrometry*, **2013**, 354-355, 281-287.
21. J. S. Becker, M. V. Zoriy, M. Dehnhardt, C. Pickhardt and K. Zilles, *Journal of Analytical Atomic Spectrometry*, **2005**, 20, 912-917.
22. M. V. Zoriy, M. Dehnhardy, G. Reifenberger, K. Zilles and J. S. Becker, *International Journal of Mass Spectrometry*, **2006**, 257, 27-33.
23. M. V. Zoriy, M. Dehnhardt, A. Matusch and J. S. Becker, *Spectrochimica Acta Part B*, **2008**, 63, 375-382.
24. D. Hare, S. Tolmachev, A. James, D. Bishop, C. Austin, F. Fryer and P. Doble, *Analytical Chemistry*, **2010**, 82, 3176-3182.
25. O. Reifschneider, C. A. Wehe, K. Diebold, C. Becker, M. Sperling and U. Karst, *Journal of Analytical Atomic Spectrometry*, **2013**, 28, 989-993.
26. J. S. Becker, A. Gorunoff, M. Zoriy, A. Izmer and M. Kayser, *Journal of Analytical Atomic Spectrometry*, **2006**, 21, 19-25.
27. J. Kaiser, M. Galiova, K. Novotny, R. Cervenka, L. Reale, J. Novotny, M. Liska, O. Samek, V. Kanicky, A. Hrdlicka, K. Stejskal, V. Adam and R. Kizek, *Spectrochimica Acta Part B*, **2009**, 64, 67-73.
28. B. Wu, M. Zoriy, Y. Chen and J. S. Becker, *Talanta*, **2009**, 78, 132-137.
29. B. Wu, Y. Chen and J. S. Becker, *Analytica Chimica Acta*, **2009**, 633, 165-172.

30. A. B. Moradi, S. Swoboda, B. Robinson, T. Prohaska, A. Kaestner, S. E. Oswald, W. W. Wenzel and R. Schulin, *Environmental and Experimental Botany*, **2010**, 69, 24-31.
31. B. Wu, I. Susnea, Y. Chen, M. Przybylski and J. S. Becker, *International Journal of Mass Spectrometry*, **2011**, 307, 85-91.
32. P. M. Outridge, G. Veinott, R. D. Evans, *Environ. Rev.*, **1995**, 3, 160-170.
33. S. F. Durrant, N. I. Ward, *J. Anal. Atom. Spectrom.*, **2005**, 20, 821-829.
34. J. S. Becker, J. S. Becker, M. V. Zoriy, J. Dobrowlska, A. Matusch, *Eur. J. Mass Spectrom.*, **2007**, 13, 1-6.
35. J. S. Becker, A. Matusch, B. Wu, *Anal. Chim. Acta*, **2014**, 835, 1-18.
36. Vogel, A.; Venugopalan, V. *Chem. Rev*. **2003**, 103, 577-644.
37. H. Reinhardt, M. Kriews, H. Miller, O. Schrems, C. Ludke, E. Hoffmann, J. Skole, *Fresen. J. Anal. Chem.*, **2001**, 370, 629-636.
38. R. Kessel, P. Ulmer, T. Pettke, M. W. Schmidt, A. B. Thompson, *Am. Mineral.*, **2004**, 89, 1078-1086.
39. G. F. Verbeck, W. D. Hoffman. *US Pat.*, US8586943 B2, **2012**.
40. J. Feldman, A. Kindness, P. Elk, *J. Anal. Atom. Spectrom.*, **2002**, 17, 813-818.
41. M. Aerts, A. C. Hack, E. Reusser, P. Ulmer, *Am. Mineral.*, **2010**, 95, 1523-1526.
42. J. S. Becker, M. V. Zoriy, C. Pickhardt, N. Palomero-Gallagher, K. Zilles, *Anal. Chem.*, **2005**, 77, 3208-3216.
43. M. V. Zoriy, M. Kayser, A. Izmer, C. Pickhardt, J. S. Becker, *Int. J. Mass Spec.*, **2005**, 242, 297-302.
44. I. Konz, B. Fernandez, M. L. Fernandez, R. Pereiro, A. Sanz-Medel, *Anal. Chim. Acta*, **2014**, 809, 88-96.
45. R. Hannigan, T. Darrah, F. Peri, *US Pat.*, WO2014152898 A3, **2014**.
46. P. J. White, E. J. Veneklaas, Plant Soil, **2012**, 357, 1-8.
47. H. Marschner, *Mineral Nutrition of Higher Plants*, Academic Press, London, 2nd edn., **1995**, 313-404.

48. J. S. Hamilton, E. L. Gorishek, P. M. Mach, D. Strutevant, M. L. Ladage, N. Suzuki, P. A. Padilla, R. Mitler, K. D. Chapman, G. F. Verbeck, *J. Anal. At. Spectrom.,* **2016**, 31, 1030-1033.

CHAPTER 4

COLD LA-ICP-MS AND RAMAN IMAGING OF PRONG GILLED MAYFLY (EPHEMEROPTERA: LEPTOPHLEBIIDAE)

4.1 Introduction

The Róbalo River, located on Navarino Island in the Cape Horn Biosphere Reserve, runs through the Dientes of Navarino Range, provides drinking water to Puerto Williams and empties into the beagle channel. Puerto Williams is the world's southernmost town and Capital of the Chilean Antarctic Province. With one of the lowest human population densities within temperate latitudes, a lack of terrestrial connectivity, and industrial and urban development the entire Sub-Antarctic Magellanic ecoregion, which houses the Róbalo River, remains relatively untouched. The biodiversity of the area remains unique as the topographic and climatic barriers isolate the biome from the nearest tropical forests. Most of the research conducted in the area of study omits the smaller organisms such as the fresh-water macroinvertebrates due to the difficulty to study such organisms.[1]

In order to introduce simple methods of analysis two imaging techniques, Raman and LA-ICP-MS, were used to study the prong-gilled mayfly (Ephemeroptera: Leptophlebiidae) sourced from the Róbalo River. Both Raman and LA-ICP-MS offer relatively simple methods of analysis and the data gathered can be presented in an easy to understand format in the way of imaging. Both techniques have been used in previous studies of non-vertebrate. Raman spectroscopy has been performed on chitin and chitosan,[2,3] insect inclusions in Baltic and Mexican amber resins,[4] the globin found in

Aphrodite aculeate,[5] and even the meiofauna of the mangrove swamps of Guadeloupe.[6] LA-ICP-MS imaging has been previously performed on slugs,[7,8] water fleas,[9] bees,[10] and amphipoda.[11]

4.2 Method

4.2.1 Sample prep

When collected, the mayflies were stored in industrial grade ethanol in a glass vial. To prepare for imaging analysis the mayflies were rinsed with 18.2MΩ H2O then embedded in 10% (w/v) porcine gelatin in 18.2MΩ H2O. -80°C for 24 hours and transferred to -20°C for 72 hours to equilibrate. Sections were cryo-cut with a Leica CM1950 at -18°C at 50µm and thaw mounted on 18x18mm 1 ounce glass coverslips which range from 0.13–0.17mm thickness. Sequential slices from the same mayfly which had best retained shape were selected for analysis.

4.2.2 Raman Imaging Procedure

The coverslip mounted sample is placed on the inverted microscope and a 4000 µm by 1000 µm area is selected with a 10 µm step size. The coverslip is thin enough to not case interference in the Raman Spectra. The imaging is then performed at ambient temperature with an iHR550 Raman Imaging Spectrometer with Synapse detector and 785nm laser source which was first aligned with a Si standard. A range of 1600 to 1700 cm^{-1} peak is selected in the Labspec software and a XYZ color map of intensity is generated and then correlated back to the bright field image.

4.2.3 Laser Ablation Inductively Coupled Mass Spectrometry Imaging Procedure

The sample-mounted coverslip is placed on top of the Peltier device and locked into the ablation chamber so that an air tight seal is formed. The water pump is turned on so that the ice cold water begins to flow through the heat sink and a voltage of about 1.0 V is applied to the Peltier device. As the temperature is allowed to stabilize the carrier gas, helium, is flowed through the chamber at a rate of 1000 mL/min as to prevent condensation buildup on the window of the chamber. A line scanning raster pattern is set up to cover the entirety of the mayfly from top to bottom and the Z position of the ablation pattern is determined by utilizing the UP-213's CCD camera to focus on the sample. ICP and Laser settings were set according to Table 2. A XYZ color map of each element is then generated from the intensity data obtained.

ICP Parameters		Laser Settings	
Rf Power	1.5 kW	Wavelength (nm)	213
Plasma Flow	16.5 L/min	Ablation mode	Line by line
CRI Flow	40 mL/min, Skimmer	Repetition Frequency (Hz)	20
Analytes	^{57}Fe, ^{66}Zn, ^{65}Cu	Number of Passes	1
		Energy output	75%
Analysis Mode	Semi-Quantitative, Time resolved, Peak hopping	Spot diameter (μm)	40
		Scan speed (μm/s)	80
		Distance between lines	75

Table 2: Laser and ICP parameters and settings used in this experiment.

4.3 Results/Discussion

4.3.1 Raman Image

The chosen wavelength range for the image was 1600 - 1700 cm^{-1}, which includes the δ(NH) band in chitin at 1626 cm^{-1} (Figure 6). Along with the image the spectra at a point on the edge of the invertebrate is included (Figure 7, 8). The spectra labeled for chitin includes the peaks 460 cm^{-1}, 498 cm^{-1} [δ(CO-NH) + δ(C-CH_3)], 955 cm^{-1} [**ν**(CN)], 1414 cm^{-1}, and 1626 cm^{-1} [δ(NH)]. All of which are common peaks for chitin.[12,13] Along with the chitin peaks present there were several monosaccharide and polysaccharide

peaks such as D-(+)-Xylose, D-(-)-Fructose, and Amylose The sample remained undamaged by the process of imaging.[13]

4.3.2 Laser Ablation Inductively Coupled Mass Spectrometry Images

In order to limit the amount of polyatomic interferences, which is a common issue with elements such as Fe, the CRI was utilized during analysis. ^{66}Zn and ^{65}Cu were found to be dispersed throughout the body of the mayfly with higher counts towards the head (Figure 9 A,B). ^{57}Fe had low counts throughout the body but a high count localization towards the midgut region of the insect (Figure 9 C). With little human interaction to the Róbalo river area, the likely source of metals introduction to the river water would be from the volcanic rock of the mountains. Run off water and snow has been found to have higher than 100 ppb concentrations of Fe and 10-100 ppb concentrations of Cu and Zn.[14] It is possible that metal uptake occurred during the invertebrate's life in the Róbalo River.

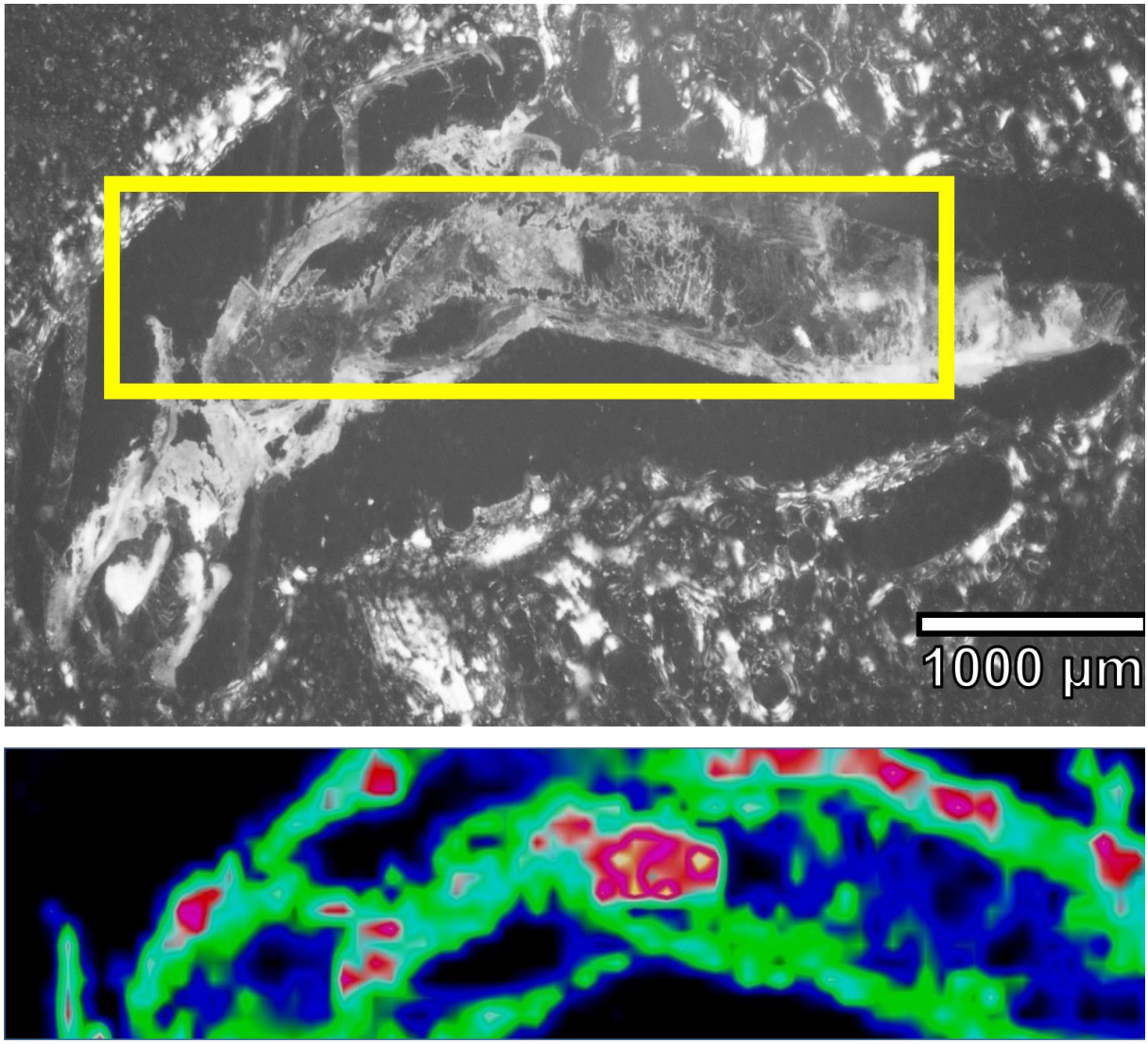

Figure 6: Bright field image of the mayfly with area selected for Raman imaging blocked out. As well as the Raman image at the selected wavelength range (1600-1700 cm^{-1})

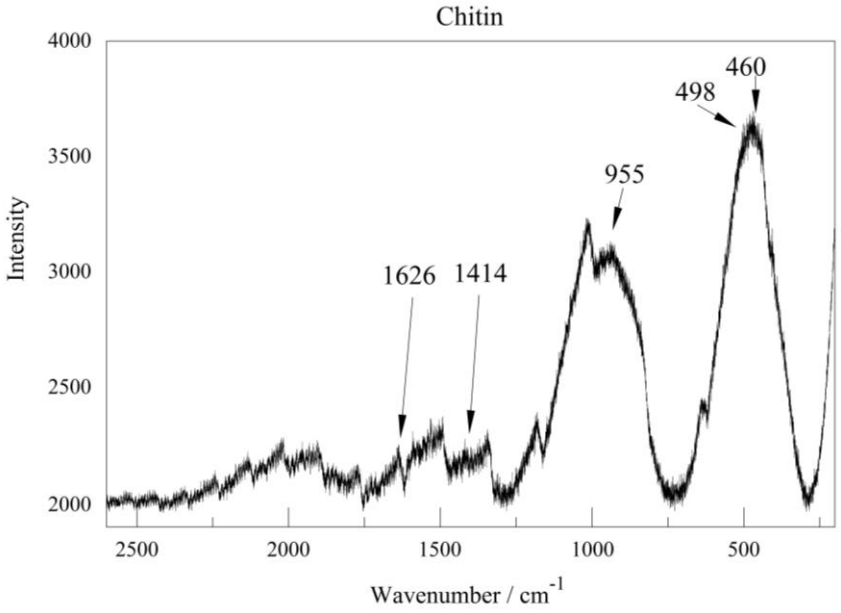

Figure 7: Raman spectra of chitin peaks from point on the edge of the sample

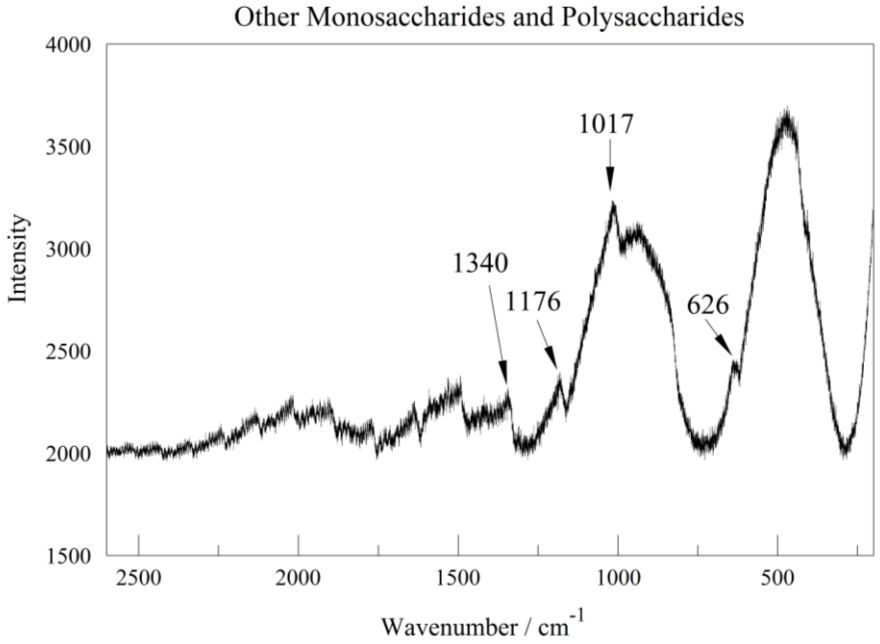

Figure 8: Assigned peaks for other mono- and polysaccharides found at same point.

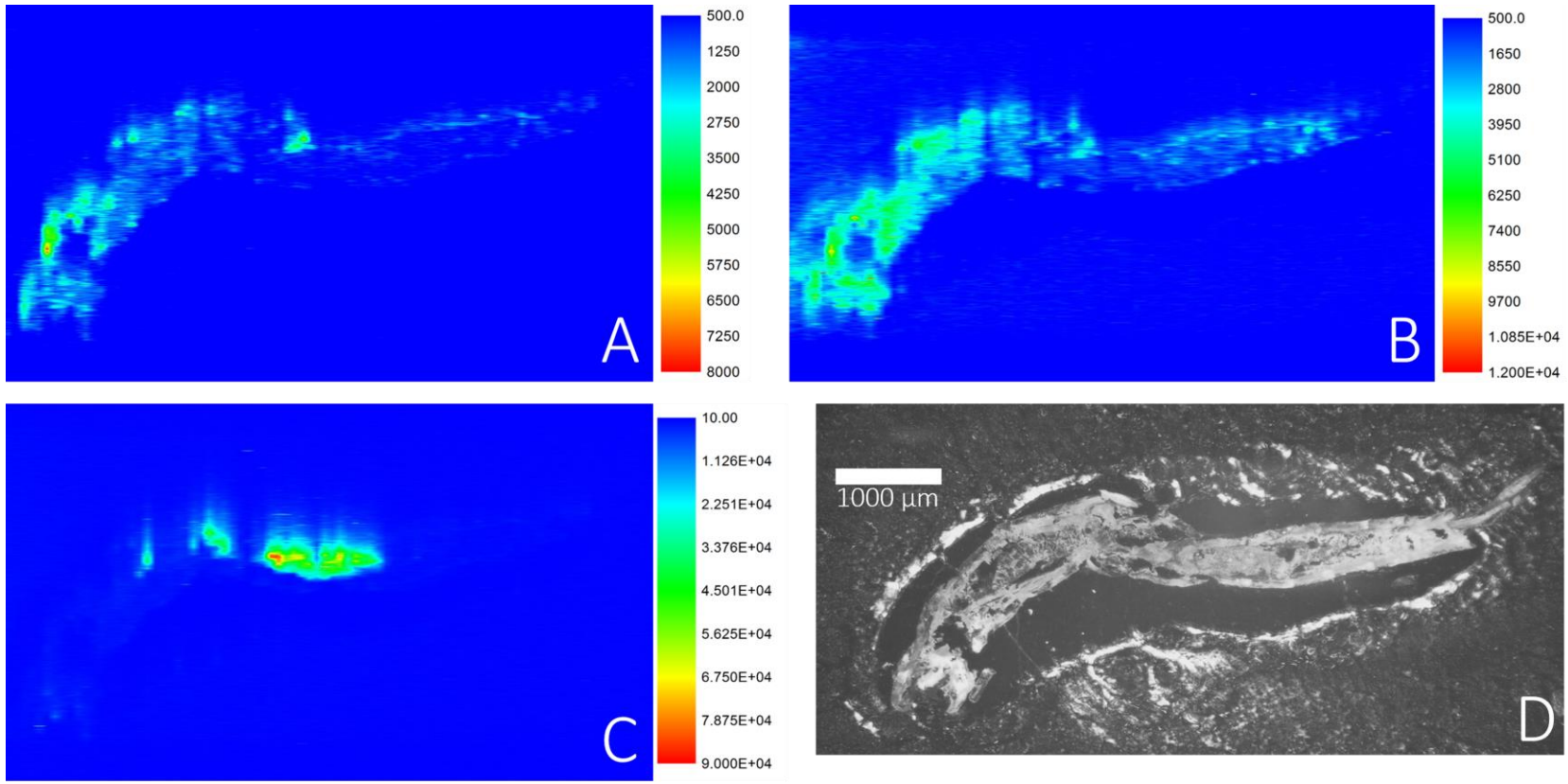

Figure 9: (D) Bright field image of mayfly sample. (A) Contour intensity map of ^{65}Cu, (B) Contour intensity map of ^{66}ZN, and (C) Contour intensity map of ^{57}Fe.

4.4 Conclusion

In order to demonstrate Raman and LA-ICP-MS as useful instruments for imaging studies in entomology a prong-gilled mayfly from the Róbalo River in Chile was analyzed. Both techniques demonstrate an ease of use, provide information on environmental factors, and provide visualization of the physiology of the invertebrate. While LA-ICP-MS is destructive, Raman is not. In future studies it would be beneficial to use LA-ICP-MS to provide quantitative information. To do so a matrix matched standard of the elements would need to be included on the coverslip and analyzed along with the sample. Another hope for future work would be to further optimize the laser settings to lessen the destructive nature of the ablation. Finally, it would be beneficial to further study more imaging instrumentation for the scope of entomology.

4.5 References

1. T. A. Contador Mejias, *Benthic Macroinvertebrates of Temperate, Sub-Antarctic Streams: The Effects of Altitudinal Zoning and Temperature on the Phenology of Aquatic Insects Associated to the Robalo River, Navarino Island (55°S), Chile* [Online], The University of North Texas, Denton, TX, **December 2011**.
2. A. Zając, J. Hanuza, M. Wandas, L. Dymińska, *Spectrochimica Acta Part A: Molecular and Biomolecular Spectroscopy*, **2015**, 134, 114-120.
3. C. V. Serrano, H. Leemreize, B. Bar-On, F. G. Barth, P. Fratzl, E. Zolotoyabko, Y. Politi, *Journal of Structural Biology*, **2016**, 193, 124-131.
4. H. G.M. Edwards, D. W. Farwell, S. E. J. Villar, *Spectrochimica Acta Part A: Molecular and Biomolecular Spectroscopy*, **2007**, 68, 1089-1095.
5. K. Ramser, W. Wenseleers, S. Dewilde, S. Van Doorslaer, L. Moens, D. Hanstorp, *Journal of Biochemical and Biophysical Methods*, **2007**, 70, 627-633.
6. L. C. Maurin, D. Himmel, J. Mansot, O. Gros, *Marine Environmental Research*, **2010**, 5, 382-389.
7. J. S. Becker, A. Matusch, C. Depboylu, J. Dobrowolska and M. V. Zoriy, *Analytical Chemistry*, **2007**, 79, 6074-6080.
8. J. S. Becker, D. Pozebon, A. Matusch, V. L. Dressler and J. S. Becker, *International Journal of Mass Spectrometry*, **2011**, 307, 66-69.
9. D.S. Gholap, A. Izmer, B. De Samber, J.T. van Elteren, V.S. Selih, R. Evens, K. De Schamphelaere, C. Janssen, L. Balcaen, I. Lindemann, L. Vincze, F. Vanhaecke, J.S. Becker, *Analytica Chimica Acta*, **2010**, 664, 19–26.

10. T.H. Wang, C.H. Jian, Y.K. Hsieh, F.N. Wang, C.F. Wang, *Journal of Agricultural and Food Chemistry*, **2013**, 61, 5009–5015.
11. B.P. Jackson, D. Bugge, J.F. Ranville, C.Y. Chen, *Environmental Science and Technology*, **2012**, 46, 5550–5556.
12. A. Zając, J. Hanuza, M. Wandas, L. Dymińska, *Spectrochimica Acta Part A: Molecular and Biomolecular Spectroscopy*, **2015**, 134, 114-120.
13. J. De. Gelder, K. De Gussem, P. Vandenabeele, L. Moens, *Journal of Raman Spectroscopy*, **2007**, 38, 1133-1147.
14. K. V. Ragnarsdottir, S. R. Gislason, T. Thorvaldsson, A. J. Kemp, A. Andresdottir, *Mineralogical Magazine*, **1994**, 58A, 752-753.

CHAPTER 5

CONCLUSIONS AND FUTURE WORK

5.1 Summary of Work

LA-ICP-MS and Raman are both powerful instruments for imaging of biological samples. LA-ICP-MS is capable of detecting pictogram concentrations of trace metals and can be beneficial for the stud of environmental effects on organisms. Raman is a non-destructive method of analysis. Both instruments have simple sample prep and can even work with little to no sample prep dependent on the sample.

With the *B. napus* seeds the importance of a cold cell system for LA-ICP-MS imaging of biological samples was studied. A custom peltier based cold cell system was developed in house to fit the UP-213 laser ablation system. It was evident that ablating at ambient temperatures caused heating to occur in the sample. This heating caused further break down of the sample leading to an increase and longer carry over of the signal. This effect on the signal caused inaccurate images which appeared to blur. By keeping the sample cool with the cold cell the transient signal had little to no carry over, which in turn lead to cleaner and more accurate images.

The benefit of Raman and LA-ICP-MS imaging for entomology was studied by the analysis of prong-gilled mayfly from the Róbalo River in Chile. Raman imaging revealed the chitin make-up throughout the invertebrate and highlighted the physiological sections of the invertebrate. As well as revealed the presence of other monosaccharides and polysaccharides. LA-ICP-MS imaging of the invertebrate unveiled the localization of ^{57}Fe to the midgut region, which is likely from intake of the fresh water which runs from the volcanic rock of the Dientes of Navarino Range.

5.2 Future Work

Currently the work performed on these subjects was qualitative or semi-quantitative at best. In future studies it would be beneficial to do quantitative analysis. This can easily be done with LA-ICP-MS by the inclusion of matrix matched standards in the form of a gradient on the same coverslip the sample is mounted on. Another goal for future work in LA-ICP-MS imaging would be to decrease the spot size for greater resolution while still maintaining proper ablation and image quality or even increasing the image quality. It would also be beneficial to optimize the laser settings further in an effort to lessen the destructive nature of laser ablation. This could also be achieved by choosing hardier samples as well as thicker sections when cryo-cutting. Lessening the destructive nature would then allow for samples imaged by LA-ICP-MS to further be analyzed by other imaging instrumentation or chemical analysis techniques.